Radial Modulation of Microbubbles for Ultrasound Contrast Imaging

Ayache Bouakaz, *Member, IEEE*, Michel Versluis, Jerome Borsboom, and Nico de Jong, *Associate Member, IEEE*

***Abstract*—Over the past few years, extensive research has been carried out in the field of ultrasound contrast imaging. In addition to the development of new types of ultrasound contrast agents, various imaging methods dedicated to contrast agents have been introduced, and some of them are now commercially available. In this study, we present results of an imaging technique that is capable of detecting echoes from microbubbles and eliminating those emanating from nonoscillating structures (tissue), thereby enhancing contrast imaging. The method is based on mixing a low frequency (LF) modulator signal and a high frequency (HF) imaging signal to effectively modulate the size of the contrast microbubble through its volumetric oscillations using the LF signal and to probe the radial motion using the HF imaging signal. To evaluate the performances and limitations of the method, high-speed optical observations and acoustic measurements were carried out on soft-shelled microbubbles. The results showed that, by incorporating the modulator signal, the bubbles respond differently compared to the HF excitation alone. The decorrelation between the signals obtained at the compression and expansion phase of the modulator signal is significantly high to be used as a parameter to detect contrast microbubbles and discriminate them from tissue. The echo received from a solid reflector shows identical responses during the compression and rarefaction phase of the LF signal. In conclusion, these results demonstrate the feasibility of this fully linear approach for improving the contrast detection.**

I. Introduction

Ultrasound contrast agents (UCAs) are indicated in radiology and cardiology for various applications, such as left ventricular opacification and enhanced endocardial border delineation [1]. However, substantial research efforts are still undertaken to use UCA for the assessment of myocardial perfusion. The first generation of contrast agents was composed of free air bubbles, but newer generations consist of encapsulated microbubbles of gas that are sufficiently stable to pass into the systemic circulation following injection into a peripheral vein. These bubbles contain either air or a low solubility gas to lower the diffusion rate and, hence, increase their lifetime in the blood. Most of these agents are intended to enhance the echo from the blood pool. In combination with novel imaging techniques, second generation contrast agents have significantly improved the delineation of blood vessels in both conventional B-mode and Doppler-mode imaging. Over the past few years, extensive research has been carried out in the field of ultrasound contrast imaging. In addition to the development of new generations of ultrasound contrast agents, various imaging methods dedicated to contrast agents have been introduced, of which some are commercially available. Imaging methods such as pulse inversion [2]–[4] and power modulation [5] are now effectively used to image contrast microbubbles in various clinical applications and already show significant success in many clinical situations. However, these methods have shown limited success in detecting myocardial perfusion during echocardiographic examinations, especially with "difficult-to-image" patients. Therefore, new imaging methods are investigated based on the unique acoustic properties of gas microbubbles [6]–[8]. The ultimate detection technique should be able to ascertain suppression of the strong (linear or nonlinear) tissue echoes while increasing the bubbles echoes. Therefore, the discrimination between nonperfused tissue and contrast-perfused tissue usually is expressed in the contrast-to-tissue ratio. Numerous detection methods have been proposed in the literature and are all based on the specific acoustic signatures of microbubbles [8]–[11].

The method described in this paper is capable of selectively detecting echoes from contrast microbubbles while reducing or eliminating echoes emanating from nonoscillating structures such as tissue. It is based on mixing two frequency components: a low frequency (LF) signal, which is used as a modulator signal, and a high frequency (HF) signal, which is used as an imaging signal. The LF signal modulates the size of the bubbles through acoustically driven vibration. The HF signal is superimposed onto the LF signal and interrogates the modulated bubbles or, in other words, images the local radial oscillations of the gas bubbles as induced by the LF signal. This approach was initially proposed by Deng *et al.* where they applied a dual frequency technique to study phenomena associated with ultrasound contrast agent bubbles [12]. They carried out ultrasonic measurements using the dual-frequency band technique to explore contrast agent dynamics, destruction, and modifications in the medium properties, e.g., the speed of sound. Information regarding the concentration of the microbubbles as well as their size was extracted using the

Manuscript received June 12, 2006; accepted July 14, 2007.

A. Bouakaz is with Inserm U619, Tours, France, and also with the Université F. Rabelais, Tours, France (e-mail: bouakaz@med.univ-tours.fr).

M. Versluis and N. de Jong are with Physics of Fluids, University of Twente, Enschede, The Netherlands.

J. Borsboom is with and N. de Jong is also with the Department of Biomedical Engineering, Erasmus MC, Rotterdam, The Netherlands.

N. de Jong is also with the Interuniversity Cardiology Institute of the Netherlands, Utrecht, The Netherlands.

Digital Object Identifier 10.1109/TUFFC.2007.532

HF signal. Additionally, they investigated the change of the microbubble sizes due to the LF signal as detected by the HF signal.

In this paper, we experimentally explore the capabilities of this method for ultrasound contrast imaging and discuss its limitations in terms of sensitivity. Time-resolved optical observations using an ultra high-speed camera were performed while exploring the effects of excitation signals on individual microbubbles. In addition, acoustic measurements were carried out on a bulk solution of a commercially available contrast agent to evaluate its performance in the case of a wider distribution of microbubble sizes. These acoustical results were compared to those obtained using a solid reflector. Parts of this work were described in a proceedings paper [13] and a Ph.D. thesis [14].

II. Method Description

The acoustic pressure generated from the modulator signal will vary the size of the bubbles, depending on its phase. An insonified contrast bubble will be small during the compression phase of the modulator signal and large during the rarefaction phase. Due to the strong nonlinear nature of contrast bubbles, the varying bubble size can be detected with the HF imaging signal, i.e., the response of the bubble to the imaging signal will differ between the positive and negative cycles of the modulator signal. The response of linear scatterers to the imaging signal will be identical in both phases of the modulator signal as predicted by the superposition principle. This difference in response can be exploited to differentiate between contrast bubbles and tissue. Although tissue cannot be considered linear at the full pressure range used for diagnostic ultrasound imaging, the typical pressures used for contrast imaging are low enough to cause minimal, nonlinear effects in tissue. In addition, the LF modulator signal may induce a strong phase shift in the HF response when the instantaneous resonant frequency of the bubble is alternatingly modulated above and below the frequency of the HF imaging signal. Such a phase shift, although not studied at present, may prove to be important to further enhance the sensitivity of the radial modulation imaging method described here.

To illustrate the principle of the method, Fig. 1 shows the diameter-time (DT) curve of a 4 μm diameter SonoVue (Bracco Research SA, Geneva, Switzerland) microbubble simulated using a modified Rayleigh-Plesset equation [15]. The microbubble was insonified with one cycle of a 0.5 MHz modulator signal and three cycles of a 3.5 MHz imaging signal at 135 kPa and 185 kPa peak pressure, respectively. Microbubble shell properties used in the simulation were taken from Gorce *et al.* [16], [17]. The imaging signal was transmitted during the maximum compression and rarefaction phases of the modulator signal as this is where we expect the largest difference in the size of the bubble. The simulated DT-curve shows that the microbubble compresses to almost 3 μm during the first half cycle

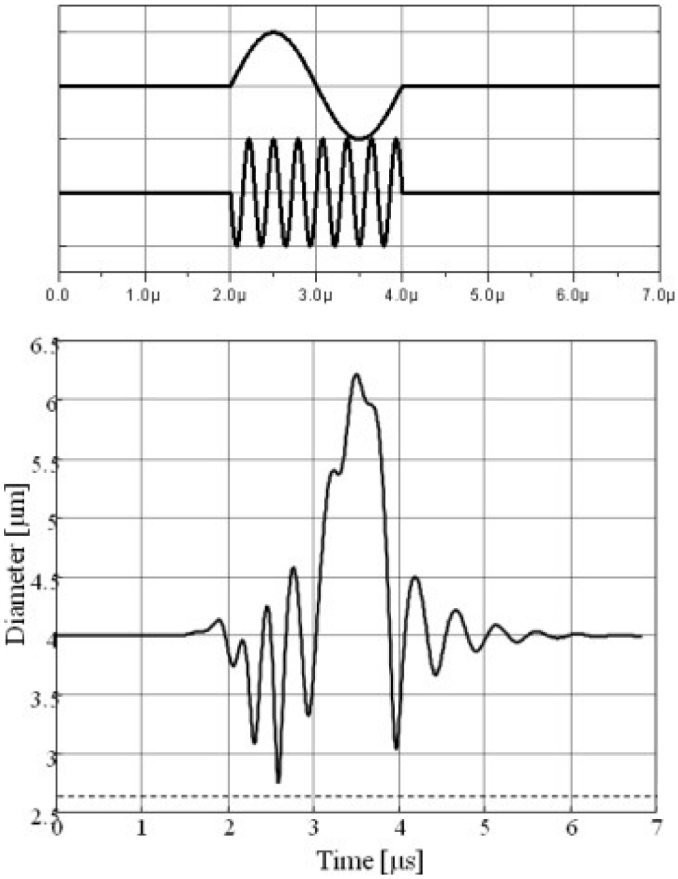

Fig. 1. Simulated DT curve of a 4-μm diameter SonoVue bubble excited with one cycle of a 0.5 MHz, modulator signal at 130 kPa peak negative pressure and seven cycles of a 3.5 MHz, imaging signal at 185 kPa.

of the modulator signal, which is close to its theoretical 3.5 MHz resonant diameter of 2.7 μm, and expands to approximately 6 μm during the second half cycle of the modulator signal. The simulated curve shows that the bubble responds stronger to the imaging signal when it is compressed than when it is expanded, and that the difference is large enough to be exploited in a microbubble detection technique.

III. Experiments

A. Optical Measurements

To evaluate the performance and sensitivity of dual-frequency insonification in differentiating between gas bubbles and tissue, optical observations were carried out with the Brandaris-128 high speed camera system [18]. This system is capable of digitally acquiring 128 frames with a maximum frame rate of 25 million frames-per-second. To insonify the bubbles at significantly different frequencies, two single-element, broadband transducers focused at 75 mm with center frequencies of 0.5 MHz and 3.5 MHz were used. They were perpendicularly mounted in a Perspex container and positioned such that their focal dis-

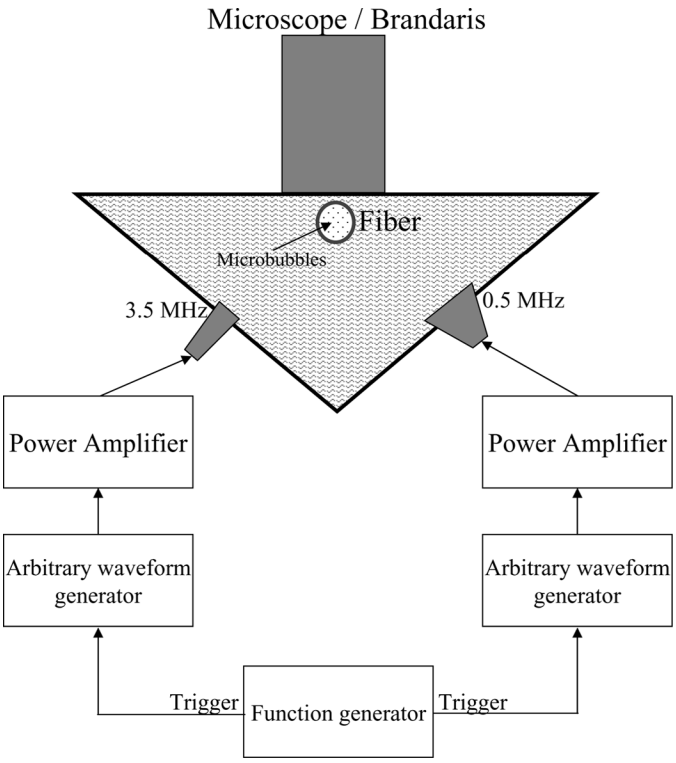

Fig. 2. Experimental optical setup.

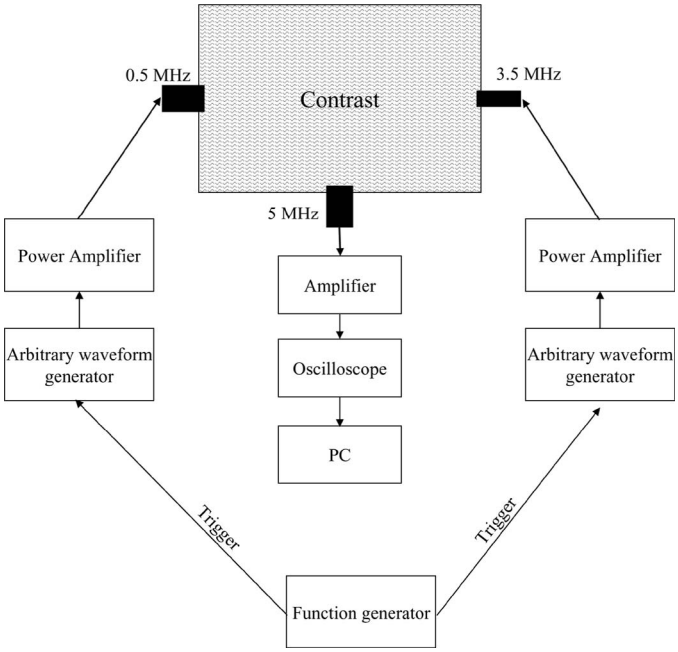

Fig. 3. Experimental acoustical setup.

tances intersected at a depth of 75 mm as depicted in Fig. 2. Both transducers were mounted under an angle of 45° relative to the top of the block. A synthetic Cuprophan® capillary fiber (Akzo Nobel Faser AG, Wuppertal, Germany) with an inner diameter of 160 μm was placed horizontally and, hence, perpendicularly to both ultrasound beams in the focus of the transducers. A microscope objective was positioned above the capillary fiber that projected images of the contrast agent bubbles with 120 times magnification onto the high-speed camera. Electrically gated excitation signals of 6 cycles at 0.5 MHz and 40 cycles at 3.5 MHz were generated by arbitrary waveform generators (33220A, Agilent, Santa Clara, CA). The pressure amplitude was adjusted by two separate, variable attenuators (355C/D, HP, Palo Alto, CA), and it was amplified using two linear power amplifiers (2100L, ENI, Rochester, NY, and 150A100B, AR, Souderton, PA). In this way, the acoustic pressures delivered to the contrast bubble could be controlled independently for each frequency and chosen so as to avoid microbubble disruption [19]. A function generator was used to trigger both waveform generators and to ascertain that modulator and imaging pressure waves coincided at the focal points of the transducers.

A flow of 1:1000 diluted SonoVue (Bracco Research SA, Geneva, Switzerland) microbubbles was driven through the fiber by manually pressing the syringe connected to the fiber to move fresh bubbles into the region of interest. The flow was stopped by releasing the pressure. The bubbles under investigation remained in view for several hundred milliseconds. All optical experiments described in this paper were carried out at a precisely measured frame rate of near 14 million frames per second; 128 successive frames were recorded for each experiment.

The applied acoustic peak negative pressures were measured in a separate experiment using a calibrated hydrophone (Precision Acoustics, Dorset, UK). Both the objective and the capillary fiber were removed from the Perspex container and the tip of the hydrophone was positioned at the point at which the fiber had crossed the ultrasound beams. The acoustic peak negative pressures were 120 kPa and 180 kPa at 0.5 MHz and 3.5 MHz, respectively, which corresponds to mechanical indices of 0.17 and 0.10. This indicates that we operated in a nondestructive regime for the contrast agent.

B. Acoustical Measurements

Acoustical measurements were performed with the very same transducers used in the optical experiments in a modified setup to accommodate a third receiving transducer, see Fig. 3. A solution of SonoVue bubbles with a 1:2000 dilution was used in these experiments in order to improve the signal-to-noise ratio. The two transmit transducers were installed at opposite sides of the setup, and they were carefully aligned in such a way that their acoustical axes coincided. The modulator signal consisted of an untapered burst of 20 cycles at 0.5 MHz and 40 kPa peak negative pressure. This signal was synchronized with an imaging signal that consisted of an untapered burst with a variable number of cycles at 3.5 MHz and 50 kPa peak negative pressure. Both transducers were electrically driven by the same setup as the optical experiments. Echoes from the microbubbles were recorded passively with a broadband 5 MHz transducer. The transducer was focused at 75 mm and was positioned perpendicularly to the beams

of the two transmitting transducers. The received echo signals were amplified (AU-3A-0110, Miteq, Hauppage, NY) and digitized with a Lecroy digital oscilloscope (9400A, LeCroy, Chestnut Ridge, NY) and transferred to a computer for further analysis. The analysis was performed on tenfold averaged time traces to increase the signal-to-noise ratio of the recorded traces.

IV. Results

A. Optical Observations

Fig. 4(a) shows a recording obtained with the high-speed camera. The top image shows a microscopic image of the microbubbles in the region of interest before insonification. The bubble that has been selected as the bubble under investigation is indicated by the arrow. In the bottom panel, the diameter-time curve of this bubble is shown during simultaneous insonation with the modulator and the imaging signal. It is shown that the 3.5 MHz imaging signal is already present at the beginning of the recording, and the 0.5 MHz modulator signal starts to show its effects at about 2 μs. At this point, we see that the resulting DT curve of the bubble consists of a HF component superimposed on a LF component, although not in a linear fashion. The HF component is visible during the compression phase of the bubble while it is much less pronounced during the expansion phase. Fig. 4(b) shows the Fourier power spectrum of the DT curve. It shows two dominant peaks of about 0.5 MHz and 3.5 MHz, which correspond to the modulator and imaging signals, respectively. The other peaks correspond to the saw-tooth shaped window that is implied by the delayed arrival of the modulator signal and the rectangular window that is implied by the effect of the modulator signal on the amplitude of response to the imaging signal. These last points are made more clear in Fig. 5, which shows the DT curve after band-pass filtering at 0.5 MHz (dotted lines) and 3.5 MHz (solid lines). We observed that up to 3 μs, the 0.5 MHz oscillation of the microbubble was relatively weak due to the recent arrival of the 0.5 MHz wave and the corresponding gradual build-up of the 0.5 MHz oscillations of the bubble. As we can see from the solid curve, these variations in size are too small to cause a significant difference in bubble response at 3.5 MHz, which is relatively constant between the compression and expansion phases of the 0.5 MHz component. Beyond 3 μs, the amplitude of the 0.5 MHz oscillations gradually increase giving rise to a bubble size of approximately 3 μm in the compression phase and 6 μm in the expansion phase. The interaction of the modulation signal with the 3.5 MHz imaging signal is well visible. Starting from 3 μs, the 0.5 MHz oscillations are large enough to give a significant difference in the amplitude of the 3.5 MHz oscillations for the different phases of the 0.5 MHz oscillation. During the expansion phase of the 0.5 MHz component of the bubble, the 3.5 MHz component decreases in amplitude, and during the compression phase of the 0.5 MHz

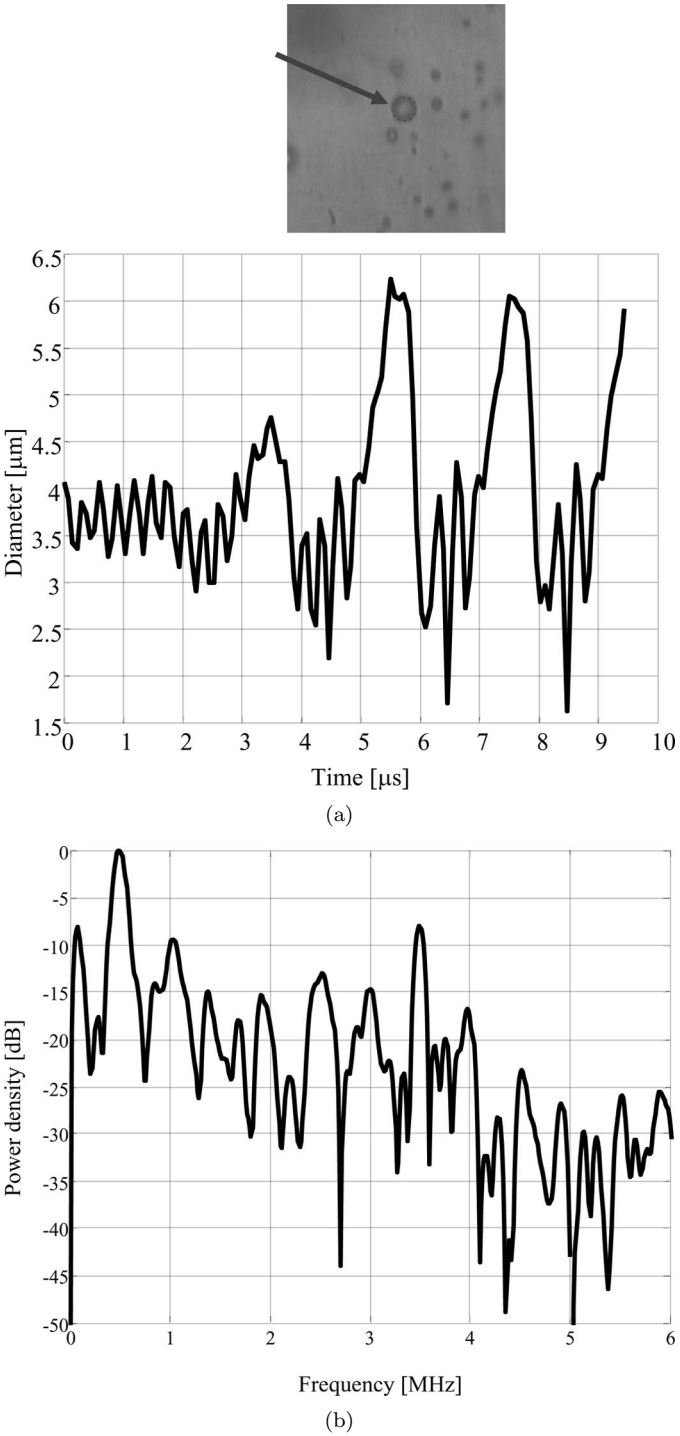

Fig. 4. (a) Top image, optical image of SonoVue bubbles in the region of interest in which the bubble under investigation is indicated by an arrow. Lower graph, DT curve of a 4-μm diameter SonoVue microbubble insonified with a double frequency signal (0.5 MHz and 3.5 MHz) as extracted from an optical recording acquired through ultra high-speed imaging. (b). Fourier spectrum of the DT curve of the 4-μm diameter SonoVue microbubble shown in Fig. 4(a).

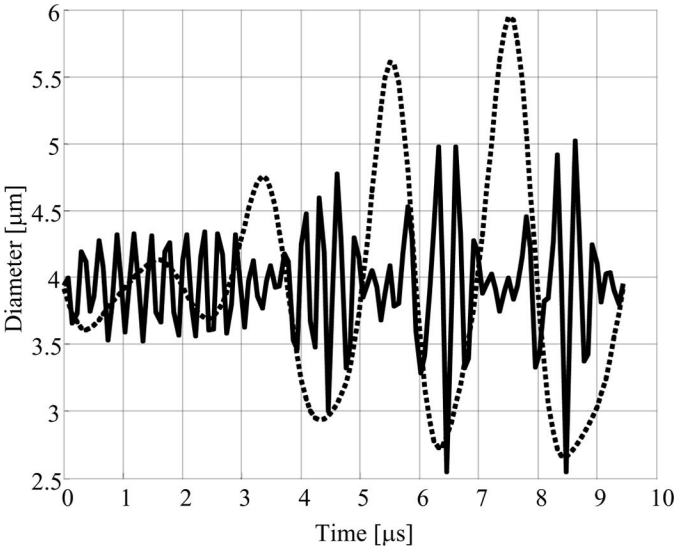

Fig. 5. Frequency separated DT curves at 0.5 MHz (dotted lines) and 3.5 MHz (solid lines) of a 4-μm diameter SonoVue microbubble insonified with a double frequency signal (0.5 MHz and 3.5 MHz).

component of the bubble the 3.5 MHz component increases in amplitude.

The difference in the 3.5 MHz response of the bubble for the compression and expansion phases of the 0.5 MHz response can be explained by considering the instantaneous resonance frequency of the bubble. The 0.5 MHz modulator signal changes the instantaneous bubble size from 3 μm and 6 μm. The resonance frequency of a SonoVue bubble for these sizes is 3.5 MHz and 1.7 MHz, respectively [20]. As the imaging signal is at 3.5 MHz, we are imaging the bubble approximately at resonance when it is in its compression phase of the 0.5 MHz component. Consequently, we expect the 3.5 MHz radial response in this case to be larger in the compression phase than in the expansion phase, which agrees with our optical observations.

The different responses of the 3.5 MHz imaging signal during the opposite phases of the modulator signal allow for an efficient detection of contrast bubbles embedded in structures that are not sensitive to radial modulation, for example, tissue. The expected contrast enhancement was estimated from the power ratio of the 3.5 MHz signal responses during these two modulator phases. Pc is defined as the power of the 3.5 MHz filtered R-t signal (see Fig. 5) during the bubble compression phase, and Pr is defined as the power during the bubble expansion phase. Both signals were of the same length in time. The signal enhancement then was calculated as $10 * \log_{10}$ (Pc/Pr). In this example, the enhancement was approximately 15 dB.

B. Acoustical Measurements

Radial modulation measurements also were performed in an acoustic setup. To ascertain spatial overlap between the LF modulator signal and the HF imaging signal at the intersection of the transmit beams with the receive beam, the excitation signals consisted of long waveforms.

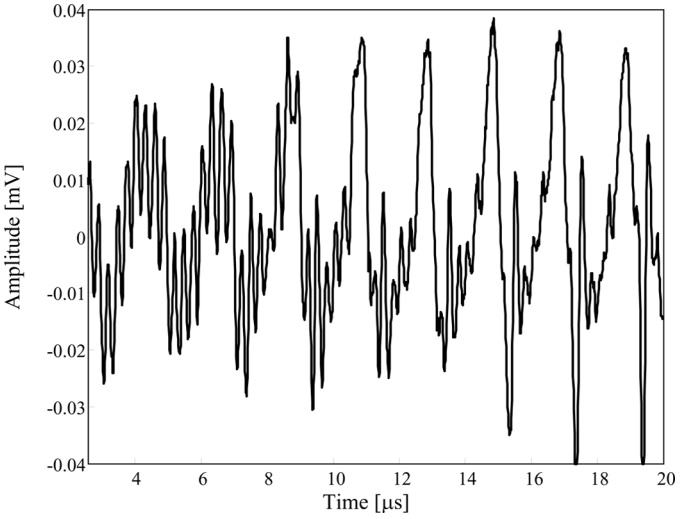

Fig. 6. Acoustical response of a suspension of SonoVue microbubbles insonified with a double frequency signal (0.5 MHz and 3.5 MHz).

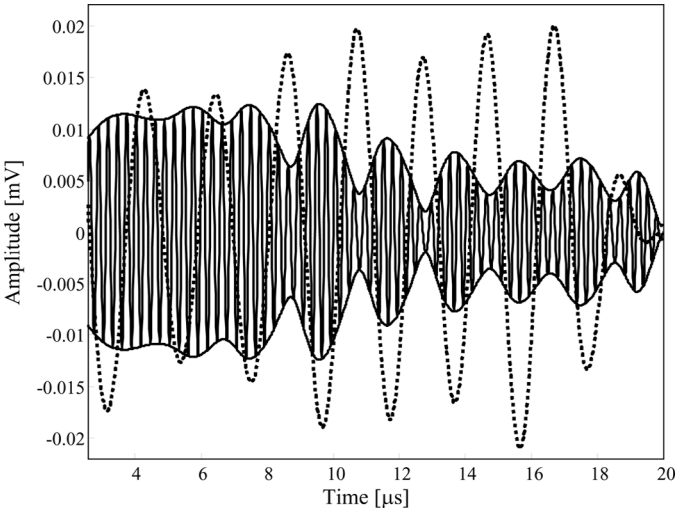

Fig. 7. Frequency separated acoustical response at 0.5 MHz (dotted lines) and 3.5 MHz (solid lines) of a suspension of SonoVue microbubbles insonified with a double frequency signal (0.5 MHz and 3.5 MHz).

Fig. 6 shows an example of a recording in which both signals consisted of bursts of 20 cycles. The curve shows the bulk response averaged over 10 time traces to increase the signal-to-noise ratio. The 0.5 MHz modulator component is visible in the recorded signal. Up to 8 μs, no difference is observed in the 3.5 MHz response between the compression and rarefaction phases of the modulator signal. Beyond 8 μs, the difference is more apparent. The band pass filtered 0.5 MHz and 3.5 MHz components of the trace in Fig. 6 are displayed in Fig. 7. The curves confirm that, during the start of the recorded signal, the echo at 3.5 MHz does not show a significant difference for the phases of the modulator signal. Beyond 8 μs, the 3.5 MHz component is strongly present during the negative half-cycle of the modulator signal, and its amplitude is decreased during the positive half-cycle.

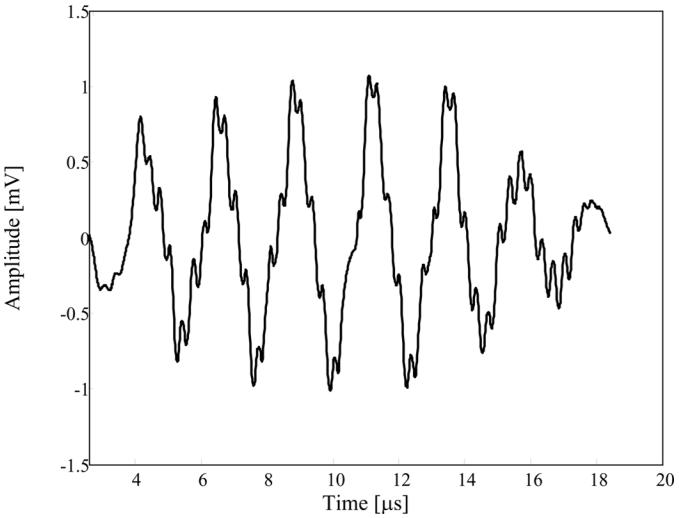

Fig. 8. Acoustical response of a solid, flat reflector insonified with a double frequency signal (0.5 MHz and 3.5 MHz).

In a separate experiment, we confirmed that, for linear structures—represented by a solid reflector—the HF response is identical during the compression and expansion phases of the modulator signal. A recorded trace of this experiment, which used the same acoustic settings as the bulk contrast acoustic experiment, is shown in Fig. 8. The contrast enhancement also was estimated from the acoustical data of the bubble response in Fig. 6 and from the data of the solid reflector in Fig. 8 by calculating the ratio of the signal power during the compression and expansion phases of the modulator signal. The estimated contrast enhancement was 0.6 dB for the flat solid reflector and 17.4 dB for the contrast agent suspension.

V. Discussion

The results presented in this study are based on the application of a modulator signal that induces a change in the instantaneous contrast bubble properties, which then is detected with a HF imaging signal. Because this scheme only works when applied to a nonlinearly reacting structure, it can be applied to differentiate between the echoes from linear structures (e.g., tissue) and nonlinear structures (e.g., contrast bubbles). It is important to note that the oscillatory nature of a bubble is not the important factor in this technique. A linear oscillator will never show a difference in the response of the imaging signal when whatever signal is superimposed on that signal. When applied to a bubble, the effect of the modulator signal is twofold. First, the resonance frequency of the bubble strongly depends on its radius. Therefore, when the frequency of the imaging pulse is adjusted to the bubble size, the resonance frequency of the bubble can be shifted toward and away from the imaging frequency and, hence, influence the amount of radial excursion of the bubble as the radial excursion of a bubble is maximal around its resonance frequency. This effect was shown in the optical recordings. Second, the size of the bubble will influence its scattering efficiency. A larger bubble will generate a stronger pressure wave than a smaller bubble when oscillating with equal radial excursion. This effect was included in the acoustic experiments and also may explain why the effect is so well pronounced in the acoustical experiments in which it is applied to an ensemble of bubbles with different sizes. When the frequencies are properly chosen, the modulator signal will, in its expansion phase, shift the peak of the size distribution to a size in resonance with the imaging frequency. This will have the effect that a large amount of bubbles are close to resonance and, thus, their responses will dominate the reflected echo signal.

The absence of an interaction between the modulator signal and imaging signal up to 8 μs in Fig. 7 possibly can be explained by the absence of bubbles that are insonified by both the modulator and the imaging signal. As can be seen in Fig. 3, the modulator pressure wave is coming in from the left, and the imaging pressure wave is coming in from the right. Up to 8 μs, the respective wave fronts have not yet passed each other. Therefore, none of the bubbles are simultaneously excited by both pressure waves. The received echo signal then is just a linear superposition of echoes from bubbles excited by either only the modulator signal and echoes from a different set of bubbles that are excited by only the imaging signal. Consequently, there can be no interaction. Beyond 8 μs, the wave fronts have passed each other, and the interaction between modulator and imaging signal starts to become visible in the received echo trace. The change in amplitude can be explained by the wave fronts not passing each other exactly in the center of the receive beam.

In the acoustical experiments, an ensemble of contrast bubbles were insonified. For bulk contrast agent, the total response is a superposition of the contributions from individual microbubbles, some of which may not be sensitive to an interaction of the modulator signal and imaging signal. This then may degrade the sensitivity of the method. However, for a given size distribution and excitation frequency, the response will in general be dominated by bubbles around a specific size as described by Gorce *et al.* [16]. Therefore, we assume that, in the acoustical experiment, the measured effect is accountable to a specific part of the bubble population that shows the interaction between the modulator and imaging signal and dominates the returned echo.

The experimental results described in this paper demonstrate the principle and the feasibility of the radial modulation imaging approach, which is aimed at improving the discrimination between echoes originating from contrast bubbles and echoes originating from tissue. The results show that this method has advantages, but also that it has some limitations as well. As already mentioned in the acoustical results, bulk contrast agent contains a distribution of microbubble sizes, which, in general will reduce the sensitivity of the method in an acoustic setup compared to the results obtained from optical observation of a single contrast microbubble. Therefore, contrast agent

with a narrow size distribution such as those proposed by Talu *et al.* [21] and Bohmer *et al.* [22] would be best suited to exploit this approach. For commercially available contrast agents with a wide size distribution, we assume that a specific part of the contrast agent dominates the total acoustical response, and thus, we could tailor the frequencies used in this method or the size distribution of the agent to improve the sensitivity of the method. To obtain the largest difference between the compression and expansion phases of the modulator signal, we would propose to select the frequency of the imaging so that it equals the resonance frequency of the peak of the size distribution in the expansion phase. We then benefit from both the increased acoustical response due to the resonance of a large number of bubbles and the increased scattering cross section caused by the expansion phase of the modulator signal as was also reported by Deng *et al.* [12]. In the compression phase, the acoustic response of those bubbles will be considerably lower, maybe even to the point at which a different part of the size distribution dominates the response. This would increase the decorrelation between the phases of the modulator signal even more and, hence, the detectability of the bubbles.

Another application of this technique could be envisioned when the modulator signal is used to shift the entire size distribution to a range at which a larger part of the size distribution responds to the imaging signal, and hence, improves the contrast response. No separate detection step would be necessary, and it even could be performed adaptively in real time.

VI. Conclusions

The availability of new generations of ultrasound contrast agents has stimulated extensive research and developments during the last decade. Microbubble-based contrast agents have unique acoustical characteristics that differ strongly from those of tissue. Exploitation of these characteristics has led to rapid progress in the field of contrast agent specific imaging methods. Some of these methods have shown to be beneficial for native tissue imaging as well.

The optical observations as well as the acoustical measurements presented in this study show the feasibility of using a separate ultrasound signal at a low frequency to modulate the bubble size while simultaneously imaging the bubble at standard or even higher frequencies. This method still has many unexplored potentials and should be investigated further with the objective of suppressing tissue echoes while detecting the bubble echoes.

References

[1] B. B. Goldberg, J. S. Raichlen, and F. Forsberg, *Ultrasound Contrast Agents: Basic Principles and Clinical Applications*. 2nd ed. London: Martin Dunitz, 2001.

[2] D. Hope Simpson, P. N. Burns, and M. A. Averkiou, "Techniques for perfusion imaging with microbubble contrast agents," *IEEE Trans. Ultrason., Ferroelect., Freq. Contr.*, vol. 48, pp. 1483–1494, 2001.

[3] R. Schlief, "Ultrasound contrast agents," *Curr. Opin. Radiol.*, vol. 3, pp. 198–207, 1991.

[4] P. N. Burns, "Instrumentation for contrast echocardiography," *Echocardiography*, vol. 19, pp. 241–258, 2002.

[5] R. J. Eckersley, C. T. Chin, and P. N. Burns, "Optimising phase and amplitude modulation schemes for imaging microbubble contrast agents at low acoustic power," *Ultrasound Med. Biol.*, vol. 31, pp. 213–219, 2005.

[6] A. Bouakaz, S. Frigstad, F. ten Cate, and N. de Jong, "Super harmonic imaging: A new technique for improved contrast detection," *Ultrasound Med. Biol.*, vol. 28, pp. 59–68, 2002.

[7] W. T. Shi, F. Forsberg, A. L. Hall, R. Y. Chiao, J. Liu, S. Miller, K. E. Thomenius, M. A. Wheatley, and B. B. Goldberg, "Subharmonic imaging with microbubble contrast agents: Initial results," *Ultrason. Imag.*, vol. 21, pp. 79–94, 1999.

[8] P. J. A. Frinking, E. I. Céspedes, J. Kirkhorn, H. G. Torp, and N. de Jong, "A new ultrasound contrast imaging approach based on the combination of multiple imaging pulses and a separate release burst," *IEEE Trans. Ultrason., Ferroelect., Freq. Contr.*, vol. 48, pp. 643–651, 2001.

[9] A. Bouakaz, S. Frigstad, F. J. ten Cate, and N. de Jong, "Super harmonic imaging: A new imaging technique for improved contrast detection," *Ultrasound Med. Biol.*, vol. 28, pp. 59–68, 2002.

[10] F. Forsberg, W. T. Shi, and B. B. Goldberg, "Subharmonic imaging of contrast agents," *Ultrasonics*, vol. 38, pp. 93–98, 2000.

[11] J. M. G. Borsboom, C. T. Chin, A. Bouakaz, M. Versluis, and N. de Jong, "Harmonic chirp imaging method for ultrasound contrast agent," *IEEE Trans. Ultrason., Ferroelect., Freq. Contr.*, vol. 52, pp. 241–249, 2005.

[12] C. Deng, F. Lizzi, A. Kalisz, A. Rosado, R. Silverman, and D. Coleman, "Study of ultrasonic contrast agents using a dual frequency band technique," *Ultrasound Med. Biol.*, vol. 26, pp. 819–831, 2000.

[13] A. Bouakaz and N. de Jong, "New contrast imaging method using double frequency exposure," in *Proc. IEEE Ultrason. Symp.*, 2004, pp. 339–342.

[14] J. M. G. Borsboom, "Advanced detection strategies for ultrasound contrast agents," Ph.D. dissertation, Erasmus University, Rotterdam, The Netherlands, 2005.

[15] N. de Jong, R. Cornet, and C. T. Lancée, "Higher harmonics of vibrating gas filled microspheres. Part one: Simulations," *Ultrasonics*, vol. 32, pp. 447–453, 1994.

[16] J.-M. Gorce, M. Arditi, and M. Schneider, "Influence of bubble size distribution on the echogenicity of ultrasound contrast agents," *Invest. Radiol.*, vol. 35, pp. 661–671, 2000.

[17] J.-M. Gorce and M. Arditi, "Experimental and simulated acoustic properties of SonoVue: Predicted behavior in fundamental and harmonic imaging modes," in *Proc. Fourth Heart Centre Symp.*, 1999, pp. 80–81.

[18] C. T. Chin, C. T. Lancée, J. M. G. Borsboom, F. Mastik, M. Frijlink, N. de Jong, M. Versluis, and D. Lohse, "Brandaris 128: A 25 million frames per second digital camera with 128 highly sensitive frames," *Rev. Sci. Instrum.*, vol. 74, pp. 5026–5034, 2003.

[19] A. Bouakaz, M. Versluis, and N. de Jong, "High-speed optical observations of contrast agent destruction," *Ultrasound Med. Biol.*, vol. 31, pp. 391–399, 2005.

[20] S. van der Meer, B. Dollet, M. M. Voormolen, C. T. Chin, A. Bouakaz, N. de Jong, M. Versluis, and D. Lohse, "Microbubble spectroscopy of ultrasound contrast agents," *J. Acoust. Soc. Amer.*, vol. 121, pp. 648–656, 2007.

[21] E. Talu, K. Hettiarachchi, H. Nguyen, A. P. Lee, R. Powell, M. L. Longo, and P. A. Dayton, "A novel production method for lipid-stabilized monodisperse ultrasound contrast agents," in *Proc. IEEE Ultrason. Symp.*, 2006, pp. 1568–1571.

[22] M. R. Böhmer, R. Schroeders, J. A. M. Steenbakkers, S. H. P. M. de Winter, P. A. Duineveld, J. Lub, W. P. M. Nijssen, J. A. Pikkemaat, and H. R. Stapert, "Preparation of monodisperse polymer particles and capsules by ink-jet printing," *Colloids Surfaces A: Physicochem. Eng. Aspects*, vol. 289, pp. 96–104, 2006.

Ayache Bouakaz graduated from the University of Sétif, Algeria, from the Department of Electrical Engineering. He obtained his Ph.D. degree in 1996 from the Department of Electrical Engineering at the Institut National des Sciences Appliquées de Lyon (INSA Lyon), France.

In 1998 he joined the Department of Bioengineering at the Pennsylvania State University in State College, PA, where he worked as a postdoc for 1 year.

Since February 1999, he has been employed at the Erasmus University Medical Center, Rotterdam, The Netherlands. His research focuses on imaging, ultrasound contrast agents and transducer design. From January 2005, he has held a permanent position at the French Institute for Health and Medical Research, Inserm U619 in Tours, France, where his research interests are imaging and therapeutic applications of microbubbles.

Michel Versluis was born in the Netherlands in 1963. He graduated in Physics in 1988 from the University of Nijmegen, the Netherlands, with a special interest in Molecular Physics and Astrophysics, working in the field of far-infrared laser spectroscopy of interstellar molecular species. Later, he specialized in the application of intense tunable UV lasers for flame diagnostics resulting in a successful defense of his Ph.D. thesis in 1992. After a two year research position working on molecular dynamics at Griffith University, Brisbane, Australia, he continued to work on developing laser diagnostic techniques for internal combustion engines (Lund, Sweden) and industrial jet flames and solid rocket propellants (Delft, The Netherlands). Michel Versluis is now a lecturer at the University of Twente, the Netherlands, in the Physics of Fluids group working on the experimental study of bubbles and jets in multiphase flows and granular flows. He also works on the use of microbubbles as tools for medical diagnosis and therapy.

Jerome Borsboom was born in the Netherlands in 1975. He earned an M.Sc. degree in electrical engineering at Delft University of Technology, the Netherlands, in 1997. In May 2000, he joined the department of Experimental Echocardiography of the Thoraxcentre, Erasmus MC in Rotterdam, the Netherlands, to pursue his Ph.D. degree under the guidance of Nico de Jong. In 2005, he received his Ph.D. degree for his thesis 'Advanced detection strategies for ultrasound contrast agents' and continued working as a post-doc at Erasmus-MC. His research interests include the application of coded sequences for contrast agents and development of an interleaved array transducer.

Nico de Jong (A'97) was born in 1954. He graduated from Delft University of Technology, Delft, The Netherlands, in 1978. He received his M.Sc. degree in the field of pattern recognition. Since 1980, he has been a staff member of the Thoraxcenter of the Erasmus University Medical Center, Rotterdam, The Netherlands. At the Department of Biomedical Engineering, he developed linear and phased-array ultrasonic probes for medical diagnosis, especially compound and transesophageal transducers. In 1986 his interest in ultrasound applications shifted toward the theoretical and practical background of ultrasound contrast agents. In 1993 he received his Ph.D. degree for "Acoustic properties of ultrasound contrast agents."

Currently he is interested in the development of 3-D transducers and a fast-framing camera system. Dr. De Jong is the project leader of Technology Foundation STW and Foundation for Fundamental Research on Matter projects on ultrasound contrast imaging and drug delivery systems. Together with Folkert ten Cate, he is organizer of the annual European Symposium on Ultrasound Contrast Imaging, held in Rotterdam and attended by approximately 175 scientists from all over the world.